ECCOMAS Congress 2016
VII European Congress on Computational Methods in Applied Sciences and Engineering
M. Papadrakakis, V. Papadopoulos, G. Stefanou, V. Plevris (eds.)
Crete Island, Greece, 5–10 June 2016

A 3D ELECTROMECHANICAL FEM-BASED MODEL FOR CARDIAC TISSUE

Minh Tuan Duong[1,2], **Alexander Jung**[1], **Ralf Frotscher**[1] **and Manfred Staat**[1]

[1] Aachen University of Applied Sciences
Institute of Bioengineering
Heinrich-Mußmann-Str. 1, 52428 Jülich, Germany
e-mail: {a.jung, frotscher, m.staat}@fh-aachen.de

[2] Hanoi University of Science and Technology
DaiCoViet No.1, Hanoi, Vietnam
tuan.duongminh@hust.edu.vn

Keywords: Cardiac Tissue, Cell Models, Drug Modeling, Electromechanical Coupling

Abstract. *The CellDrum provides an experimental setup to investigate the electromechanics of a cardiac tissue construct and particularly the effect of drugs. Experimental data were used to develop a respective computational electromechanical model. Until now, the experiments have been performed with a thin tissue construct. Mechanically, it was modeled as a materially and geometrically nonlinear shell. Future experiments with thicker tissue are planned. Thus, the mechanical model needs to be modified. This study aims to predict the outcome of such experiments using a nonlinear 3D continuum formulation. Here, the action of one drug, verapamil, was taken into account.*

1 INTRODUCTION

A human heart is divided into four chambers, two atria and two ventricles, connected by four valves. The right atrium receives oxygen-poor blood from the body and pumps it to the right ventricle from where it is pumped to the lungs. The left atrium receives oxygen-rich blood from the lungs and pumps it to the left ventricle from where it is pumped back to the body. Both the filling and ejection processes are controlled by electrophysiological processes. At the cellular level the main components in the heart are cardiomyocytes, cardiac fibroblasts, endothelial cells and vascular smooth muscle cells [1]. Cardiomyocytes are subdivided into two types, namely the pacemaker-conduction and the contractile cardiomyocytes. Each cardiac cycle is initiated by sinoatrial cells located in the upper wall of the right atrium. Sinoatrial cells are pacemaker cardiomyocytes that can generate spontaneous action potentials, i.e. a rapid change in the membrane potential. Over a conduction system the action potential propagates throughout the whole heart so that the contractile cardiomyocytes in the atria and ventricles are electrically excited. Cardiomyocytes are composed of myofilaments enabling the cells to contract. Even pacemaker-conduction cardiomyocytes are able to contract but by far not as strong as the contractile cardiomyocytes. In a process called excitation-contraction coupling the action potential results in a release of Ca^{2+} from intracellular stores which activate the sarcomeres so that tension can be created and the cells can contract.

Computational cardiac models have been developed with the motivation to investigate the physiology and pathologies of the heart and ultimately to optimize therapies. In 1952, Hodgkin and Huxley published the first electrophysiological model of an excitable cell [2]. For a squid giant axon they linked the kinetics of ion channel conformation change with ion currents through the cell membrane and the change of the membrane potential. Ten years later, this groundbreaking work was extended by Noble to model the electrophysiology of cardiac myocytes [3]. Since then, the understanding of cellular mechanisms and the experimental potential has increased. This has led to the development and improvement of models for different types of human cardiomyocytes [4-7]. Since the models are already at a mature stage, they can serve as a basis to investigate the effect of various drugs on the cardiac electrophysiology [7, 8]. When these models are applied to tissues the action potential propagation from one cell to its neighboring cells needs to be taken into account. For this, the monodomain and bidomain reaction-diffusion equations are used. Bidomain equations account for the different electrical conductivities of the intracellular and extracellular spaces whereas only one conductivity is used in the monodomain equations. Differences between monodomain and bidomain results were reported to be extremely small [9] so that the monodomain equations with a much lower computational cost is widely preferred. Solving them with the Finite Element Method (FEM) gives the membrane potential averaged over a set of myocytes in each element.

While many questions can be addressed with electrophysiological models, others e.g. regarding the dilated cardiomyopathy necessitates a complete representation of the electromechanics. Improved computer performance has made it possible to develop FEM models where the electrophysiology is coupled with the mechanics. Electromechanical coupling is based on the relationship between the electrical activation of the tissue, the respective active tension generated by the sarcomeres and the resulting deformation [10]. Here, the electrophysiology is modeled on the cellular level [11-15] or is simplified using eikonal equations [16] and the FitzHugh-Nagumo model [17,18]. There exist a wide range of electromechanical models from the cell [10,12] over the tissue [14] to the organ level including left ventricular models [11,15], models of both ventricles [12-15,17], and whole heart models [18]. They feature a varying degree of complexity with respect to the anatomical representation, associated mesh fineness, boundary conditions, material models, underlying electrophysiological models and coupling

models depending on the research objective. Different from the electrophysiological models electromechanical models are still in a maturing phase. Magnetic resonance imaging makes it now possible to create patient-specific highly resolved anatomical models [13], ventricle muscle fiber directions can be determined and assigned with a rule-based algorithm [19] and the orthotropic electric [20] and mechanical properties [21, 22] of the ventricular myocardium are well studied. However, there are still many tasks towards a highly sophisticated whole heart computer model. Examples include the model parametrization and validation procedures [23].

For thin cardiac tissue constructs these tasks have been addressed with a device called *CellDrum* [24, 25]. The *CellDrum* is a multiwell with circular wells, each having a diameter of 16 mm and a bottom formed by a 4 μm thin silicone membrane. Human-induced pluripotent stem cell-derived cardiomyocytes (hiPSC-CM) are seeded and cultivated on top of the silicon membrane which is coated with fibronectin. The tissue consists of a mixture of ventricular, atrial, and nodal hiPSC-CM as well as fibroblasts (Cor.4U®, Axiogenesis AG, Germany). Together with the silicon membrane the tissue construct has a thickness of up to 19 μm. The hiPSC-CM live within a culture medium and beat autonomously. Clamped in a fixed ring the tissue construct can be inflated by a syringe pump and the contraction-dependent deflection can be measured using a laser sensor. From the time function of the deflection more parameters can be derived including the beating frequency, contraction duration, activation time, relaxation time and resting time. Microscopic analyses have shown that the cardiomyocytes are randomly distributed and thus a global electrically and mechanically isotropic behavior can be assumed [13]. Goßmann *et al*. [25] used the *CellDrum* to study the effect of various drugs and observed significant changes in the mentioned parameters. Motivated by the idea to complement experiments and to get a more detailed insight, Frotscher *et al*. [14, 26, 27] developed an electromechanical model of the thin cardiac tissue construct. The mechanical part of the thin tissue construct is modeled as a materially and geometrically nonlinear shell whereas the electrical part is modelled as a three-dimensional nonlinear continuum. On the basis of experiments the model could be parameterized, verified and validated. Simulations including the action of various drugs were in good agreement with respective experiments.

Future experiments are planned to be performed with a much thicker tissue. This study aims to roughly predict their results. For this purpose, the two-dimensional shell formulation for the mechanical part has been replaced by a three-dimensional nonlinear continuum formulation. Simulations were carried out with the focus on the time function of the deflection including the action of the drug verapamil which is most widely used for the treatment of cardiac arrhythmias.

2 ELECTROMECHANICAL MODEL

2.1 Electrophysiological model

Sinoatrial pacemaker cells located at the center of the circular tissue generate an action potential which then propagates throughout the entire tissue and trigger other autonomously depolarizing sinoatrial, ventricular and atrial cells. In the presented model it is assumed that all cells are homogeneously distributed. Action potential propagation is modelled using the monodomain equation [28]. This reaction-diffusion type parabolic partial differential equation is known as the 3D cable-equation and reads in a modified form

$$\frac{\partial V}{\partial t} = \nabla \cdot (\mathbf{D} \nabla V) - I_{src}(I_{tot}^*, C_m^*, V_m^*) \tag{1}$$

with the diffusion tensor

$$\mathbf{D} = D\mathbf{I} \tag{2}$$

in the case of isotropic propagation and the no-flux condition at the boundaries of the tissue construct

$$\mathbf{n}(\mathbf{D}\nabla \mathrm{V}) = 0. \tag{3}$$

V denotes the macroscopic potential [mV], D is the diffusion coefficient which was chosen to be 35 $\mathrm{mm^2 s^{-1}}$, $\mathbf{I}$ is the identity matrix, $\mathbf{n}$ is the outward normal of the tissue construct and I_{src} is the source current density $[\mathrm{mA(mF)^{-1}}]$. The source current density

$$I_{src} = (\theta_n I_{tot}^n + \theta_a I_{tot}^a + \theta_v I_{tot}^v)\big(1 - \theta_f\big) \tag{4}$$

originates from the homogenized microscopic total cellular membrane current densities I_{tot}^* $[\mathrm{mA(mF)^{-1}}]$ where the membrane capacity C_m^* is already included. Here, θ_* $(*= n, a, v, f)$ are volume fractions of the nodal cells (n), atrial cells (a), ventricular cells (v) and fibroblasts (f). The volume fractions in Cor.4U® hiPSC-CM are given by Axiogenesis AG as 0.05, 0.35, 0.60 and 0.25, respectively.

Hodgkin-Huxley based cell models for sinoatrial [5], atrial [6] and ventricular [4] cardiomyocytes were employed, each having the general form

$$\frac{\partial V_m}{\partial t} = -I_{tot}\,, \tag{5}$$

$$\frac{\partial g_j}{\partial t} = \alpha_j^+(V_m)\big(1 - g_j\big) + \alpha_j^-(V_m) g_j\,, \tag{6}$$

where V_m is the microscopic cell membrane potential, g_j are the gate variables of each ion channel controlling the opening and closure and α_j^+ and α_j^- are the opening and closure rates which depend on a threshold value of the membrane potential. Current densities related to the ion channel of the ion i depend on the respective gate variables and take the form

$$I_i = G_i \prod_{j=1}^{m} g_j (V_m - E_i), \tag{7}$$

where G_i is the maximum conductance and E_i is the reversal potential for the ion which flows through this channel. Summed over all n current densities and including a stimulus current density I_{stim} the total current of each cardiomyocyte type reads

$$I_{tot} = I_{stim} - \sum_{i=1}^{n} I_i. \tag{8}$$

All cell models were parametrized according to the respective original works. However, in the particular sinoatrial pacemaker cell model the maximum ion channel conductance g_{K1} was decreased from 0.0400 nSpF^{-1} to 0.0333 nSpF^{-1} resulting in an increase of beating frequency by 0.06 Hz.

Cellular interaction on the microscale level was taken into account with a simple homogenization approach. Once the total membrane current density of the sinoatrial model falls below a threshold value of 25 mA(mF)$^{-1}$, the atrial and ventricular model receive a negative stimulus current of 50 mA(mm)$^{-2}$ leading to a quick increase in membrane potential according to (5). Sinoatrial cells in turn are triggered with a stimulus current of 25 mA(mm)$^{-2}$ whenever the macroscopic potential exceeds a threshold value of −40 mV.

The employed cell models provide further ordinary differential equations for free intracellular sodium, potassium and calcium concentrations as well as for internal calcium stores that are not shown here. Electromechanical coupling is described by the following two ordinary differential equations for each cell model:

$$\frac{\partial Ca_b}{\partial t} = f_1(Ca_i, Ca_b, T), \tag{9}$$

$$\frac{\partial z}{\partial t} = f_2(z, Ca_b). \tag{10}$$

The calcium concentration Ca_b that is bound to troponin C in the myofilaments depends on the freely available calcium concentration Ca_i and on the cellular stress T being a scalar. The freely available calcium concentration is controlled by the membrane potential. Based on the calcium concentration that is bound to troponin C the strain-dependent state of activation is expressed by the activation variable $z \in (0,1)$. Finally, the cellular stress for each cell model is computed according to Niederer and Smith [10] by

$$T = T_{ref}\big(1 + \beta_0(\lambda - 1)\big)K\frac{z}{z_{max}}, \tag{11}$$

with T_{ref} being the cellular reference stress at resting length, β_0 is a scalar determining the length dependence of the isometric tension, λ is the one-dimensional cellular stretch in fiber direction, K is a velocity dependent scalar and z_{max} is the maximally available activation level. Due to a missing cell type specific parametrization an equal parametrization [10] was used for all cell types. For the whole tissue construct the cellular reference stress was determined to be $T_{ref} = 58.08{\cdot}10^{-5}$ MPa [26] which replaced the original model parameter [10].

2.2 Drug action

The antagonistic drug potency of an inhibitor can be implemented in (7) using the conductance-block formulation where the maximal conductance of the ion channel i is reduced by the factor

$$g_i = g_{i,control}\left[1 + \left(\frac{D}{IC_{50_i}}\right)^n\right]^{-1}. \tag{12}$$

Here, $g_{i,control}$ is the drug-free maximal conductance of the ion channel i, D is the drug concentration and the IC_{50} value represents the half-inhibitory value, i.e. the concentration of a given drug that will cause the current density through the channel i to be reduced by 50%. The Hill coefficient was set to n =1, i.e. one molecule of the given drug is sufficient to block one ion channel.

Several assumptions were made for the model of drug action including steady-state concentration, a homogeneous distribution and no diffusion within the tissue. It has been shown that drug effects at steady-state concentration can be well represented by this model [29]. In this study, verapamil was used which is associated with blocking effects on the hERG-, L-type calcium- and sodium-channels of the ventricular cardiomyocytes. Respective IC_{50} values and effective free therapeutic plasma concentrations (EFTPC) used for D can be found in [8]. No diffusion of the drug was considered and a homogeneous concentration was assumed.

2.3 Mechanical model

Cardiac tissue constructs using the *CellDrum* consist of a silicon membrane and the actual cardiac tissue which in turn includes various cardiomyocytes and fibroblasts. Stresses occur in two forms: passive stresses arise from the silicon membrane, the fibroblasts and the cardiomyocytes and active stresses arise from contractions of cardiomyocytes. Voigt´s isostrain condition was applied and Hill´s muscle model [30] was employed to represent the mechanical response of the cardiomyocyte mixture. Hill´s model is constituted by an active element and two passive elements, one in series and one in parallel. The passive element in series reflects the passive stress in a contraction which, however, is small compared to the produced active stress and is thus neglected.

The total mechanical response of the tissue construct can be derived by the active strain or the active stress approach. The active strain approach utilizes a multiplicative split of the deformation gradient into passive $\mathbf{F}_\mathrm{p}$ and active deformation $\mathbf{F}_a$

$$\mathbf{F} = \mathbf{F}_p \mathbf{F}_a, \tag{13}$$

whereas in the active stress approach the total stress in the tissue is additively decomposed into the passive and active stress. Since the experimental parametrization was based on the level of stresses, the latter approach was used here. Viscoelastic effects were neglected and the incompressible neo-Hookean strain energy function

$$\psi = C_{10}(I_1 - 3) \tag{14}$$

was used with a material parameter C_{10} and the first invariant I_1 of $\mathbf{B}$, the left Cauchy-Green tensor. Based on the volume fractions θ_* for the various components of the tissue construct (s: silicon membrane, t: cardiac tissue) the Cauchy stress reads

$$\begin{aligned}\boldsymbol{\sigma} = \boldsymbol{\sigma}_p + \boldsymbol{\sigma}_a = \theta_s 2J^{-1}\mathbf{B}\frac{\partial \psi^s}{\partial \mathbf{B}} - p\mathbf{I} \\ + \theta_t\left(\theta_e 2J^{-1}\mathbf{B}\frac{\partial \psi^f}{\partial \mathbf{B}} + \sum_{*=n,a,v}\theta_* 2J^{-1}\mathbf{B}\frac{\partial \psi^*}{\partial \mathbf{B}} + T^*(\mathrm{t})\mathbf{I}\right).\end{aligned} \tag{15}$$

J is the determinant of the deformation gradient, t is the time, T is the active stress described in (11), p is the hydrostatic pressure and $\mathbf{I}$ is the identity tensor,

All passive parts were taken together and in pressure-deflection tests one passive material parameter $C_{10} = 0.0838284$ MPa for the whole tissue was determined. Based on that the 2nd Piola-Kirchhoff stress $\mathbf{S}$ is given as

$$\mathbf{S} = \mathbf{S}_p + \mathbf{S}_a = 2\frac{\partial \psi}{\partial \mathbf{C}} - p\mathbf{C}^{-1} + T(t)\mathbf{C}^{-1}, \tag{16}$$

in terms of the right Cauchy-Green tensor $\mathbf{C}$.

2.4 Finite Element Models and Solution algorithm

Finite element models were created for 19 µm and 100 µm thick cardiac tissue constructs. Model specifications are given in Table 1. Mechanical and electrical models are denoted with M and E, respectively. Due to symmetry only one quarter of the *CellDrum* was modeled.

Table 1: Finite element models.

Model	Formulation		Element type	Element number
1: 19 µm	M:	2D nonlinear shell	7-node quadratic triangular	120
	E :	3D nonlinear continuum	10-node quadratic tetrahedral	7664
2: 19 µm	M:			
	E :	3D nonlinear continuum	10-node quadratic tetrahedral	7664
3: 100 µm	M:			
	E :	3D nonlinear continuum	10-node quadratic tetrahedral	7639

In the first step, the inflation process is simulated by applying a certain pressure to the clamped mechanical mesh. For the 2D-19 µm shell model, $1.8 \cdot 10^{-5}$ MPa is necessary to deflect the central point of the first model to 1.2 mm. This has been experimentally validated [14]. Displacements are then projected onto the 3D electrical mesh. Subsequently, the autonomous cell contractions are simulated using an algorithm to solve the electromechanical problem which is described in [14]. When using the same mesh for the mechanical and the electrical part, the displacements no longer need to be projected. The open source code *Code_Aster* was used to solve the nonlinear mechanical and electrical problem, whereas the cellular ordinary differential equations were solved internally using a fourth-order singly-diagonally implicit Runge-Kutta method.

3 RESULTS AND DISCUSSION

Figure 1 shows the central node deflection of both 19 µm thick cardiac tissue construct models as a function of time after the inflation process. For the inflation to 1.2 mm the same pressure of $1.8 \cdot 10^{-5}$ MPa was used for both models. The maximum central node deflection of the 3D model is 90% of the maximum central node deflection of the 2D shell model and the time course is similar in both models. The difference can be explained by a slightly higher stiffness of the continuum model.

A five times higher pressure of $9.5 \cdot 10^{-5}$ MPa is needed to inflate the 100 µm cardiac tissue construct model to the same position. After the inflation both models exhibit similar deflection-

time curves as shown in Figure 2. The higher geometrical stiffness seems to be compensated by the higher amount of contractile cardiomyocytes.

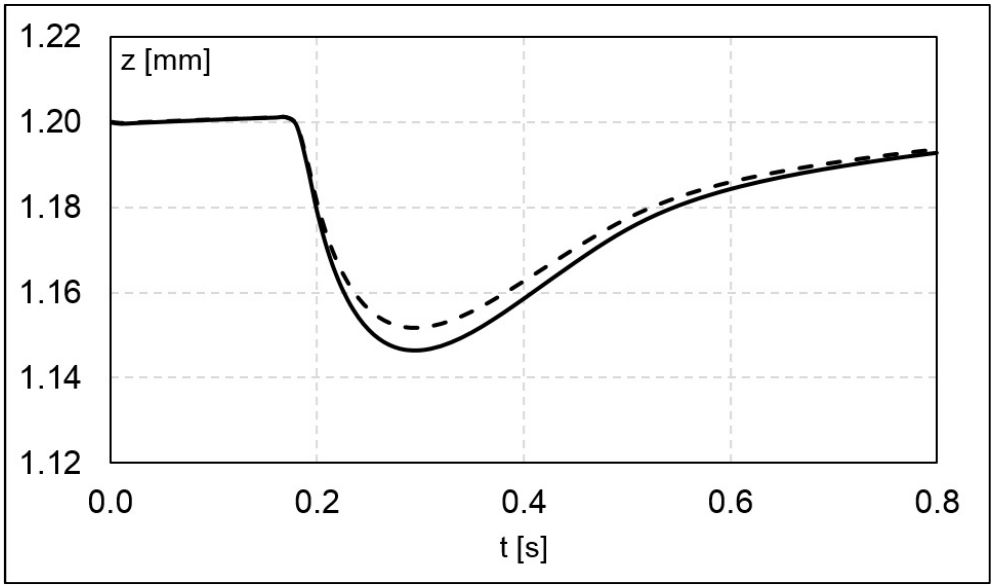

Figure 1: Central node deflection of a 19 µm thick cardiac tissue constructs after inflation. The 2D shell model (solid line) and the 3D mechanical model (dashed line) are compared. No drug was added.

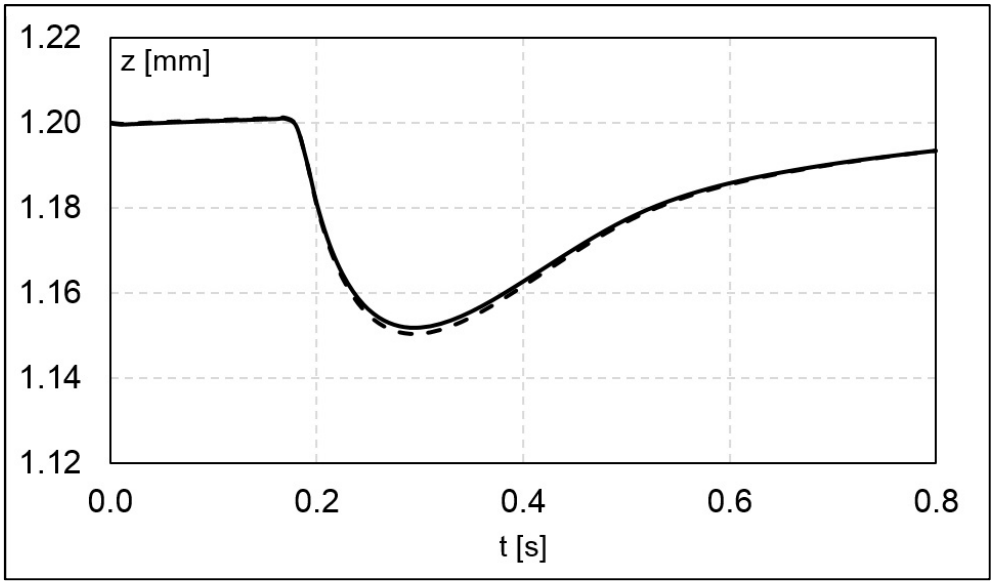

Figure 2: Central node deflection of two differently thick tissue constructs after inflation. 3D-19 µm thick (solid line) and 3D-100 µm thick (dashed line) cardiac tissue construct models are compared. No drug was added.

Verapamil was applied to the ventricular cell model [4] with a low (25 nM) and a high (81 nM) effective free therapeutic plasma concentration. The effect on the membrane potential corresponds to [8]: the duration of the action potential decreases with increasing drug concentration. As distinguished from pure electrophysiology models the presented electromechanically coupled models are capable of predicting the drug effect on the deflection. With increasing drug concentration the deflection of the tissue constructs decreases. That has already been shown experimentally using a 8 µm thick tissue construct with Cor.4U® hiPSC-CM [25] and using a simple model which contains only ventricular cells and is not based on the monodomain equation [27]. Simulations with 81 nM verapamil resulted for all models in a maximum central

node deflection which is 55% of the maximum central node deflection of the control study (Figure 3).

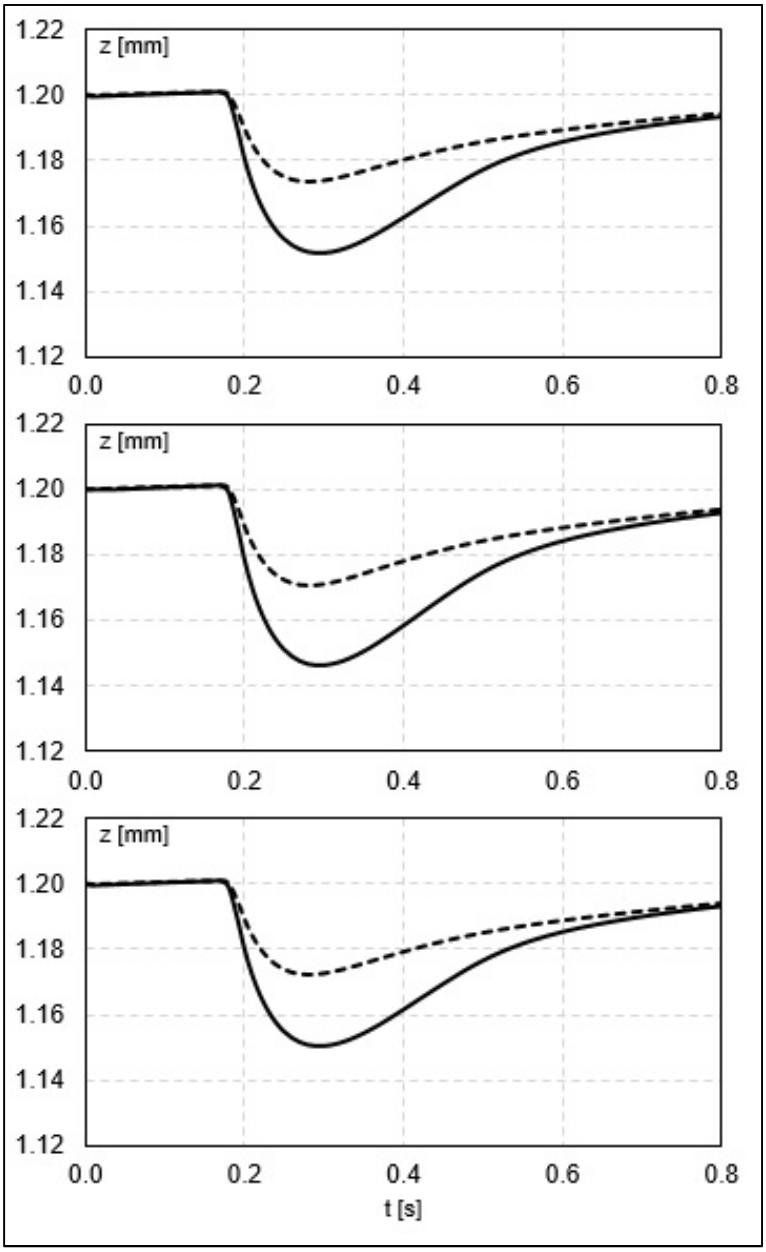

Figure 3: Effect of verapamil on the central node deflection. Results of the control (0 nM, solid line) and high EFTPC (81 nM, dotted line) are shown for all models (top to bottom: 2D-19 µm, 3D-19 µm, and 3D-100 µm).

The presented computational study shows that the time function of the deflection does not change in thicker tissue up to 100 µm. This is also true when taking into account the effect of verapamil. Experiments will be performed to derive a new parametrization and to validate these results. The aim of those models in combination with experiments is to investigate the impact of the tissue thickness on the time function of the deflection and the effect of drugs.

4 OUTLOOK

Cardiomyocytes of the left ventricle are organized in sheets with collagen fibers in between. This layered organization can be characterized with a right-handed orthonormal coordinate system with the fiber axis $\mathbf{f}_0$, the sheet axis $\mathbf{s}_0$, and sheet normal axis $\mathbf{n}_0$ (Figure 4). Throughout the ventricular wall, the sheet orientation change continuously. Orthotropic behavior has been shown for the passive mechanical response [20] and for the propagation of the action potential [20]. It has been shown that ventricular tissue is orthotropic in both electrical [20] and passive mechanical properties [21].

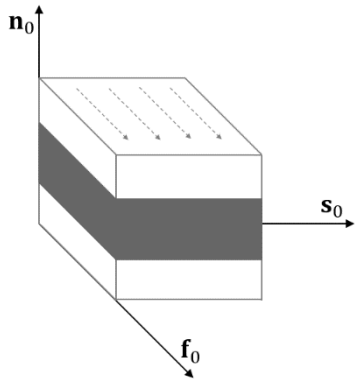

Figure 4: Layered organization of myocyte sheets and collagen fibers in between. The layered organization is characterized by a right-handed orthonormal coordinate system with fiber axis $\mathbf{f}_0$, sheet axis $\mathbf{s}_0$ and sheet normal axis $\mathbf{n}_0$.

Our ultimate goal is to develop tissue constructs and associated computational models whose results can be transferred to a certain extend to the left ventricle. So far, only tissues including a large volume of fibroblasts (25%) as well as atrial and sinoatrial cells (40% of the total cardiomyocyte volume) were available. Recently, a novel cardiomyocyte mixture has been released and thus new respective experiments are planned. The fibroblast-free mixture consists of 90% ventricular cells and just 10% atrial and sinoatrial cells (CorV.4U® Axiogenesis AG, Germany) which is a big step forward. On the basis of this novel cardiomyocyte mixture the aforementioned orthotropic nature of left ventricular tissue will be tried to take into account experimentally and computationally. Our preliminary strategy to realize this idea is explained in the remainder of this section.

So far, the cardiomyocytes have been randomly distributed on the silicon layer. Structured silicon layer should now be developed in order to align the cardiomyocytes during their cultivation. Knowing the orientation of the cardiomyocytes a computational model can be developed based on the orthotropic formulation of the action potential propagation and the passive mechanical behavior. Action potential propagation can be modelled by introducing an orthotropic diffusion tensor $\mathbf{D}$ for the monodomain equation (1). For the first instance, diffusion velocities for all three directions will be adapted from the study of Caldwell et al. (2009) [20] who examined pig left ventricular tissue. They found the maximum diffusion velocity to be in the fiber direction and the minimum diffusion velocity to be in the sheet normal direction. Unfortunately, it is not possible up to now to measure the action potential distribution within the tissue construct. The only possibility to parameterize the diffusion tensor will thus be to perform parameter studies and compare the resulting deflection-time curves with experimental data.

The orthotropic passive mechanical behavior can be modelled using the Holzapfel-Ogden strain energy function [21]:

$$\psi^{HO} = \frac{a}{2b}\exp[b(I_1 - 3)] + \sum_{i=f,s}\frac{a_i}{2b_i}\{\exp[b_i(I_{4i} - 1)^2] - 1\} + \frac{a_{fs}}{2b_{fs}}\left[\exp\left(b_{fs}I_{8fs}^2\right) - 1\right], \tag{17}$$

where a, b, a_f, a_s, b_f, b_s, a_{fs} and b_{fs} are eight positive material constants which can be derived from recent biaxial tension and triaxial shear experiments with human left ventricular tissue [22].
However, the introduction of this strain energy function require the separation of the passive stress in the silicon layer and the tissue. The neo-Hookean strain energy function ψ^{nH} will be used to model the passive mechanical behavior of the silicon membrane. Active stress in the tissue is generated in the fiber direction and the cellular reference stress can still be determined according to Frotscher et al. [26]. Employing the active stress model the 2nd Piola-Kirchhoff stress reads

$$\mathbf{S} = \mathbf{S}_p + \mathbf{S}_a = \theta_s 2\frac{\partial\psi^{nH}}{\partial\mathbf{C}} - p\mathbf{C}^{-1} + \theta_t\left(2\frac{\partial\psi^{HO}}{\partial\mathbf{C}} + T(\mathrm{t})\mathbf{F}^{-1}\mathbf{f}_0\otimes\mathbf{f}_0\mathbf{F}^{-T}\right). \tag{18}$$

Cardiac tissue models whose validated results can be transferred to the heart to a certain extend would bring numerous advantages. Drug tests could be performed with human tissue *in-vitro* which may lead to a reduction of animal experiments in cardiac drug research.

REFERENCES

[1] A.R. Pinto, A. Ilinykh, M.J. Ivey, J.T. Kuwabara, M.L. D´Antoni, R. Debuque, A. Chandran, L. Wang, K. Arora, N.A. Rosenthal, M.D. Tallquist, Revisiting cardiac cellular composition. *Circulation Research*, **118**, 400-409, 2016.

[2] A.L. Hodgkin, A.F. Huxley, A quantitative description of membrane current and its application to conduction and excitation in nerve. *Journal of Physiology*, **117**, 500-544, 1952.

[3] D. Noble, A modification of the Hodgkin-Huxley equations applicable to Purkinje fibre action and pace-maker potentials. *Journal of Physiology*, **160**, 317-352, 1962.

[4] K.H.W.J. ten Tusscher, A.V. Panfilov, Alternans and spiral breakup in a human ventricular tissue model. *American Journal of Physiology – Heart and Circulatory Physiology*, **291**, H1088-H1100, 2006.

[5] N.J. Chandler, I.D. Greener, J.O. Tellez, S. Inada, H. Musa, P. Molenaar, D. DiFrancesco, M. Baruscotti, R. Longhi, R.H. Anderson, R. Billeter, V. Sharma, D.C. Sigg, M.R. Boyett, H. Dobrzynski, Molecular architecture of the human sinus node: insights into the function of the cardiac pacemaker. *Circulation*, **119**, 1562-1575, 2009.

[6] M. Paci, J. Hyttinen, K. Aalto-Setälä, S. Severi, Computational models of ventricular- and atrial-like human induced pluripotent stem cell derived cardiomyocytes. *Annals of Biomedical Engineering*, **41**, 2334-2348, 2013.

[7] O.V. Aslanidi, M. Al-Owais, A.P. Benson, M. Colman, C.J. Garratt, J.P. Greenwood, A.V. Holden, S. Kharche, E. Kinnell, E. Pervolaraki, S. Plein, J. Stott, H. Zhang, Virtual tissue engineering of the human atrium: modeling pharmacological actions on atrial arrhythmogenesis. *European Journal of Pharmaceutical Sciences*, **46**, 209-221, 2012.

[8] G.R. Mirams, Y. Cui, A. Sher, M. Fink, J. Cooper, B.M. Heath, N.C. McMahon, D.J. Gavaghan, D. Noble, Simulation of multiple ion channel block provides improved early prediction of compounds´ clinical torsadogenic risk. *Cardiovascular Research*, **91**, 53-61, 2011.

[9] M. Potse, B. Dubé, J. Richer, A. Vinet, R.M. Gulrajani, A comparison of monodomain and bidomain reaction-diffusion models for action potential propagation in the human heart, *IEEE Transactions on Biomedical Engineering*, **53**, 2425-2435, 2006.

[10] S.A. Niederer, N.P. Smith, An improved numerical method for strong coupling of excitation and contraction models in the heart, *Progress in Biophysics and Molecular Biology*, **96**, 90-111, 2008.

[11] T.S.E. Eriksson, A.J. Prassl, G. Plank, G.A. Holzapfel, Modeling the dispersion in electromechanically coupled myocardium. *International Journal of Numerical Methods in Biomedical Engineering*, **29**, 1267-1284, 2013.

[12] R. Ruiz-Baier, A. Gizzi, S. Rossi, C. Cherubini, A. Laadhari, S. Filippi, A. Quarteroni, Mathematical modelling of active contraction in isolated cardiac myocytes, *Mathematical Medicine and Biology*, **31**, 259-283, 2014.

[13] C.M. Augustin, A. Neic, M. Liebmann, A.J. Prassl, S.A. Niederer, G. Haase, G. Plank, Anatomically accurate high resolution modeling of human whole heart electromechanics: a strongly scalable algebraic multigrid solver method for nonlinear deformation, *Journal of Computational Physics*, **305**, 622-646, 2016.

[14] R. Frotscher, D. Muanghong, G. Dursun, M. Goßmann, A. Temiz-Artmann, M. Staat, Sample-specific adaption of an improved electromechanical model of in vitro cardiac tissue, *Journal of Biomechanics*, **49**, 2016 (in press), DOI: 10.1016/j.jbiomech.2016.01.039.

[15] A. Quarteroni, T. Lassila, S. Rossi, R. Ruiz-Baier, Integrated heart – Coupling multiscale and Multiphysics models for the simulation of the cardiac function, *Computer Methods in Applied Mechanics and Engineering*, 2016 (submitted), https://www.mate.polimi.it/biblioteca/add/qmox/05-2016.pdf.

[16] M. Sermesant, R. Chabiniok, P. Chinchapatnam, T. Mansi, F. Billet, P. Moireau, J.M. Peyrat, K. Wong, J. Relan, K. Rhode, M. Ginks, P. Lambiase, H. Delingette, M. Sorine, C.A. Rinaldi, D. Chapelle, R. Razavi, N. Ayache. Patient-specific electromechanical models of the heart for the prediction of pacing acute effects in CRT: a preliminary clinical validation. *Medical Image Analysis*, **16**, 201-215, 2012.

[17] E. Berberoglu, H.O. Solmaz, S. Göktepe, Computational modeling of coupled cardiac electromechanics incorporating cardiac dysfunctions. *European Journal of Mechanics – A/ Solids*, **48**, 60-73, 2014.

[18] B. Baillargeon, N. Rebelo, D.D. Fox, R.L. Taylor, E. Kuhl, The Living Heart Project: A robust and integrative simulator for human heart function. *European Journal of Mechanics –A/ Solids*, **48**, 38-47, 2014.

[19] J.D. Bayer, R.C. Blake, G. Plank, N.A. Trayanova, A novel rule-based algorithm for assigning myocardial fiber orientation to computational heart models, *Annals of Biomedical Engineering*, **40**, 2243-2254, 2012.

[20] B.J. Caldwell, M.L. Trew, G.B. Sands, D.A. Hooks, I.J. LeGrice, B.H. Smaill, Three distinct directions of intramural activation reveal nonuniform side-to-side electrical coupling of ventricular myocytes. *Circulation: Arrhythmia and Electrophysiology*, **2**, 433-44, 2009.

[21] G.A. Holzapfel, R.W. Ogden, Constitutive modeling of passive myocardium: a structurally based framework for material characterization. *Philosophical Transactions of the Royal Society A – Mathematical, Physical and Engineering Sciences*, **367**, 3445-3475, 2009.

[22] G. Sommer, A.J. Schriefl, M. Andrä, M. Sacherer, C. Viertler, H. Wolinski, G.A. Holzapfel, Biomechanical properties and microstructure of human ventricular myocardium, *Acta Biomaterialia*, **24**, 172-192, 2015.

[23] P. Pathmanathan, R.A. Gray, Ensuring reliability of safety-critical clinical applications of computational cardiac models. *Frontiers in Physiology*, **4**, 358, 2013.

[24] P. Linder, J. Trzewik, M. Rüffer, G. Artmann, I. Digel, R. Kurz, A. Rothermel, A. Robitzki, A. Temiz-Artmann, Contractile tension and beating rates of self-exciting monolayers and 3D-tissue constructs of neonatal rat cardiomyocytes, *Medical & Biological Engineering & Computing*, **48**, 59-65, 2010.

[25] M. Goßmann, R. Frotscher, P. Linder, S. Neumann, R. Bayer, M. Epple, M. Staat, A. (Temiz) Artmann, G. Artmann, Mechano-pharmacological characterization of cardiomyocytes derived from human induced stem cells. *Cellular Physiology and Biochemistry*, **38**, 1182-1198, 2016.

[26] R. Frotscher, M. Goßmann, H.J. Raatschen, A. Temiz-Artmann, M. Staat, *Simulation of cardiac cell-seeded membranes using the edge-based smoothed FEM.* In: H. Altenbach, G.I. Mikhasev (eds), *Shell and membrane theories in mechanics and biology: From macro- to nanoscale structures*, Springer, 2015.

[27] R. Frotscher, J.P. Koch, M. Staat, Computational investigation of drug action on human-induced stem cell derived cardiomyocytes. *Journal of Biomechanical Engineering*, **137**, 071002-071002-7, 2015.

[28] J.P. Keener, J. Sneyd, *Mathematical Physiology*. New York, Springer, 1998.

[29] T. Brennan, M. Fink, B. Rodriguez, Multiscale modeling of drug-induced effects on cardiac electrophysiological activity. *European Journal of Pharmaceutical Sciences*, **36**, 62-77, 2009.

[30] A.V. Hill, The heat of shortening and the dynamic constants of muscle. *Philosophical Transactions of the Royal Society B – Biological Sciences*, **126**, 136-195, 1938.

Remark

This paper has been revised after the conference.